Acta Oceanol. Sin., 2022, Vol. 41, No. 5, P. 163–172
https://doi.org/10.1007/s13131-021-1859-2
http://www.aosocean.com
E-mail: ocean2@hyxb.org.cn

Distribution characteristics of wave energy in the Zhe-Min coastal area

Qin Ye[1], Zhongliang Yang[1], Min Bao[1, 2*], Weiyong Shi[1], Hongyuan Shi[3], Zaijin You[4], Wenyan Zhang[5]

[1] Second Institute of Oceanography, Ministry of Natural Resources, Hangzhou 310012, China

[2] State Key Laboratory of Satellite Ocean Environment Dynamics, Second Institute of Oceanography, Ministry of Natural Resources, Hangzhou 310012, China

[3] Ludong University, Yantai 264025, China

[4] Dalian Maritime University, Dalian 116026, China

[5] Institute of Coastal System, Helmholtz-Zentrum Hereon, Geesthacht 21502, Germany

Received 3 March 2021; accepted 10 May 2021

Abstract

A 10-year (2003–2012) hindcast was conducted to study the wave field in the Zhe-Min coastal area (Key Area OE-W2) located off Zhejiang and Fujian provinces of China. Forced by the wind field from a weather research and forecasting model (WRF), high-resolution wave modelling using the SWAN was carried out in the study area. The simulated wave fields show a good agreement with observations. Using the simulation results, we conducted statistical analysis of wave power density in terms of spatial distribution and temporal variation. The effective duration of wave energy in the sea area was discussed, and the stability of wave energy was evaluated using the coefficient of variation of wave power density. Results indicate that the wave energy resource in the study area was about 4.11×10^6 kW. The distribution of wave energy tends to increase from the north (off Zhejiang coast) to the south (off Fujian coast), and from near-shore area to the open sea. The sea areas with wave power density greater than 2 kW/m are mostly distributed seaward of the 10-m isobath, and the contours of the wave power density are almost parallel to the shoreline. The sea areas around the islands that are far from the mainland are rich in wave energy, usually more than 6 kW/m, and therefore are of obvious advantages in planning wave energy development and utilization. The effective duration of wave energy in the offshore area shows an increasing trend from north (off Zhejiang coast) to south (off Fujian coast), with values of ~3 500 h in the north and ~4 450 h in the south. The coefficient of variation of wave energy in this region is mostly in the range of 1.5–3.0, and gradually decreases from the north to the south, suggesting that the wave energy in the south is more stable than that in the north.

Key words: SWAN model, wave energy, wave power density, effective duration, Zhe-Min coastal area

Citation: Ye Qin, Yang Zhongliang, Bao Min, Shi Weiyong, Shi Hongyuan, You Zaijin, Zhang Wenyan. 2022. Distribution characteristics of wave energy in the Zhe-Min coastal area. Acta Oceanologica Sinica, 41(5): 163–172, doi: 10.1007/s13131-021-1859-2

1 Introduction

The shortage of fossil fuel and concern of its environmental impact have forced society to seek alternative energy sources with low impact on the environment, such as renewable and sustainable energy. As a result, many maritime countries are interested in ocean energy, especially wave energy. To make full use of wave energy before any exploitation, it requires reliable quantification of wave energy potential. Numerous wave power assessments have been conducted, including global studies (e.g., Gunn and Stock-Williams, 2012; Arinaga and Cheung, 2012) and regional studies, e.g., for coastal waters of the United States (Ahn et al., 2020), Latin American and European coastal waters (Rusu and Onea, 2019), the coastal waters of China (Wan et al., 2020), the western French coast (Gonçalves et al., 2018), the Persian Gulf (Goharnejad et al., 2021), the southwestern Black Sea coast (Bingölbali et al., 2021), the Red Sea (Aboobacker et al., 2017), Thailand (Kompor et al., 2018), Indonesia (Ribal et al., 2020), and the Philippines (Quitoras et al., 2018). Globally, the theoretical wave power is estimated to be about 2.11 Tera Watt at the 95% confidence with a buffer line running 30 nautical miles (Gunn and Stock-Williams, 2012). The total theoretical wave power along the US coasts is estimated to be approximately 2 640 Tera Watt Hours/year, roughly equivalent to 65% of American annual electricity consumption (Jacobson and Hageman, 2011). China is also a country with abundant wave power energy in both offshore and nearshore regions.

In recent years, various studies have been carried out to investigate ocean energy in China. Among them, the development and utilization of wave energy are most concerned by its society. At present, more than 10 scientific research institutions and universities in China are engaged in the development of wave energy conversion devices and technology. However, the critical technologies of reliability, survivability, and the like are still the bottleneck of wave energy technology development. The distri-

Foundation item: The National Key R&D Program of China under contract No. 2018YFB1501901; the Zhejiang Provincial Natural Science Foundation of China under contract No. LY21D060003; the Project of State Key Laboratory of Satellite Ocean Environment Dynamics, Second Institute of Oceanography, Ministry of Natural Resources, under contract Nos SOEDZZ2103 and SOEDZZ2003.
*Corresponding author, E-mail: minbao@sio.org.cn

bution of wave energy resources in each sea area has its unique characteristics. As early as the 1980s, Ma and Yu (1983), Li et al. (1984), and Wang (1984) estimated the distribution of wave energy resources in the offshore area of China using climatological and synoptic methods and measured data from offshore stations.

Observed data are, however, limited in specific regions, and they lack representativeness. With further development of wave theory and numerical techniques, more and more efforts have been dedicated to wave modeling. For example, the SWAN model (Zheng et al., 2011) and WAVEWATCH-III model (Zheng and Li, 2011) were adopted to estimate the overall spatial and temporal distribution of wave energy resources in the offshore area of China. Lin et al. (2019) evaluated wave energy in the China adjacent seas based on a 20-year SWAN hindcast. Zheng et al. (2011) and Shi et al. (2017) carried out statistical analysis of wave energy distribution along China's coasts by utilizing years of reanalysis data. Li et al. (2013), Ye et al. (2012), Zhang et al. (2012), and Wang et al. (2016a) discussed wave energy resources in local areas, including the Chengshan Cape, sea area of Fujian, offshore area of Zhejing, and sea area of Weifang based on the SWAN model, respectively.

Although many studies related to wave power have been conducted in some locations of China, comprehensive and accurate assessment of wave energy potential in the Zhe-Min coastal area has not been done. Moreover, most of these works were done using relatively low-resolution models, such as 0.5°–2.5°, which is not enough when applied to regions with complicated shorelines, such as the Zhe-Min coast. The benefit of comprehensive systematic research on wave energy resources in China is that plenty of wind and wave data have been collected at locations off China's shoreline. This national project includes four regions: OE-W1, OE-W2, OE-W3, and OE-W4 (Fig. 1a). In this study, we carried out an analysis using OE-W2 as an example.

2 Model and data

2.1 *Study area*

Our study region of OE-W2 is divided into five key areas. We will simulate each area with a high-resolution model, with attention to the complexity of shorelines (Fig. 1b). OE-W2 is located along the Zhe-Min coast in the middle of the East China Sea, with nearshore water less than 50 m deep and offshore water less than 200 m deep. Nearly every key area includes three observation stations to make sure there are good amount of data for numerical model validation. Monsoon climate of the area is characterized by the northerly wind in winter and southeasterly wind in summer.

2.2 *Wave modeling*

A three-layer nesting technique was adopted to model waves in our study area using the SWAN (Fig. 1a). The parent grid spans from 10°N to 40°N, and from 110°E to 140°E, with a spatial resolution of 0.5°×0.5°. The resolution was refined to 0.1°×0.1° in the middle layer, which was a rectangle from 24.5°N to 30°N and from 118.5°E to 123.5°E. The inner layer was nested with five small child grids (D5–D9, red boxes in Fig. 1b) at the resolution of 2′×2′. These child grids correspond to the five selected key areas

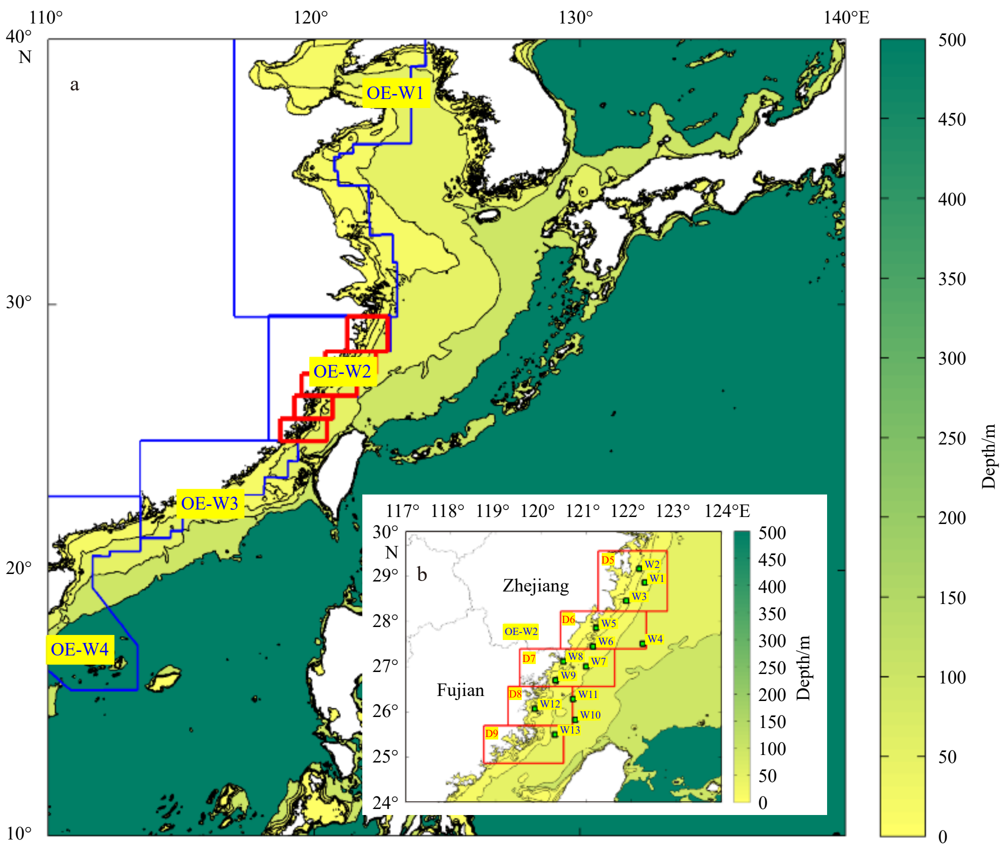

Fig. 1. Schematic of three-nested grids (a) and wave observation stations in each key area with in OE-W2 (b). Blue polygons named as OE-W1, OE-W2, OE-W3 and OE-W4 are four areas divided by the national project, here only Region OE-W2 is studied; five red rectangles named D5–D9 denote the boundaries of small child grids in the wave model; W1–W13 indicate the gauge stations.

where wave distributions under the effects of complex shoreline, topography, islands, and wind conditions are investigated in detail.

The topography and bathymetry adopted in the model were obtained by integrating the ETOP01 product with spatial resolution of 1′ and digitalized isobaths from offshore marine maps of the China Aviation Insurance Department. By combining these two data sources, the accuracy of topography and bathymetry of offshore area is ensured.

2.3 *Wind field*

In this study, hourly wind field from the WRF model for 10 successive years (2003–2012) was adopted. By assimilating the measured meteorological data from available offshore gauge stations, important parameters (e.g., wind speed and direction) were modified locally and fed to the wave model to improve odeling results of wave characteristics in the key study area. Comparison between the hindcast and measured data of W1, W4 and W10 (Fig. 1b) shows that the mean absolute error of wind speed is in the range of 1.46–1.73 m/s, and the error in simulated wind speed under normal weather conditions and cold waves is less than that under energetic weather conditions. According to some studies (Wang et al., 2011; Chen et al., 2014; Cai et al., 2019), simulation is considered to be good with absolute error less than 2 m/s or relative error less than 20%. The time range used to verify the accuracy of the input wind covers four seasons, including that from February 25, 2012 to March 26, 2012 and from June 08, 2013 to July 08, 2013 for W1, that from August 01, 2012 to August 30, 2012 and from September 18, 2012 to October 17, 2012 for W4, and that from June 17, 2012 to July 16, 2012 and from September 19, 2012 to October 18, 2012 for W10.

3 Results

3.1 *Model validation*

The measured parameters of waves at 13 observation locations within the model domain were collected to assess the model performance (Fig. 1b). Comparison between measured and modelled data shown in Figs 2 and 3 indicates that the simulated significant wave height and mean wave period are in good agreement with measured results. The correlation coefficients of significant wave height and mean wave period are 0.89 and 0.75, respectively, suggesting that the calculation results are reliable for further analysis.

3.2 *Analysis of simulated wave parameters*

The statistics of simulated significant wave height for the 10 successive years (Fig. 4a) show that the contours of mean annual significant wave height align mostly in parallel with the isobaths, increasing from shallow to deep area and from the northeast to southwest. The maximum annual average significant wave height is 1.47 m in the southeast of key area D9. Seasonal distribution of significant wave height is relatively consistent in three seasons (Figs 4b, d and e) and similar to that of mean annual significant wave height (Fig. 4a). Waves in summer (Fig. 4c) exhibit a different pattern from those in the other seasons and feature a maximum in the northeast and a gradual decrease toward the southwest. Affected by monsoon and tropical storms, waves are in general larger in winter and autumn, and the waves in the coastal area of Zhejiang is the smallest in spring, while the waves in the coastal area of Fujian is the smallest in summer.

Figure 5 shows the distribution of annual average period (Fig. 5a) is more even, and featured by the trend of increasing from the shallow to deep area; the average period is in the range of 4–5 s, and maximum average period is 5.2 s. Figure 5 shows that the average period is the longest in autumn (Fig. 5d), and the shortest in spring (Fig. 5b); and the average period in the north is longer than that in the south in summer (Fig. 5c), and the opposite is true in winter (Fig. 5e).

3.3 *Analysis of wave energy resource in key areas of OE-W2*

3.3.1 *Wave power density*

In order to investigate spatial and temporal variation of wave energy in offshore areas of Fujian and Zhejiang, power density of deep-water waves is estimated following Ma and Yu (1983):

$$P_{\mathrm{W}} = \frac{\rho g}{64\pi} {H_{\mathrm{S}}}^2 \overline{T} \approx 0.5 {H_{\mathrm{S}}}^2 \overline{T}, \tag{1}$$

where P_{W} refers to the wave power density (kW/m), H_{S} refers to the significant wave height (m) and $\overline{T}$ refers to the mean wave period (s).

By integrating the hourly significant wave height and mean wave period of 2003–2012 simulated by the model, the corresponding wave power density $P_{\mathrm{W}}(i,\ j,\ t)$ at each grid was obtained. The time-average of wave power density of each grid point was conducted to obtain the spatial distribution of average wave power density in the study area:

$$\overline{P}_{\mathrm{W}}(i,j) = \frac{1}{N}\sum_{t=1}^{N} P_{\mathrm{W}}(i,\ j,\ t), \tag{2}$$

where N refers to the accumulative time duration, representing the total number of accumulative output time steps.

Utilizing the above estimates of wave power density, we obtained the distribution of average wave power density of the 10 successive years in study sea area (Fig. 6). Results indicate that the wave power density in Zhejiang coastal area is relatively small, with the average wave power density in key area D5 of 5.3 kW/m. The wave power density in Fujian coastal area, especially in the Taiwan Strait, is the largest, with the average wave power density in key area D9 of 7.0 kW/m. The area ratio of sea area with wave power density greater than 2 kW/m suggests that there are only minor differences among different sea areas. The wave power density is mostly distributed in sea area that is relatively far from the shore. The area ratio of sea area with wave power density greater than 6 kW/m in the south is larger than that in the north; in particular, in the key Area D9 of the Taiwan Strait, it is as high as 70.3% (Table 1). As classified in Zhang et al. (2014), there are four categories for the annual wave power density with value of more than 6 kW/m, between 4 kW/m and 6 kW/m, between 2 kW/m and 4 kW/m, and less than 2, respectively. The first category of > 6 kW/m is considered to be rich in wave power density. From the power abundance view point, the resrouce in Fujian coastal region is better than that in Zhejiang coastal region. According to the distribution pattern, power-rich region is located mostly in the offshore areas, such as areas near the Dachen Island, Nanji Island, Dongtaishan Island, and Dongyin Islands. In addition, some nearshore regions along the Pingtan Island and Nanri Island are also rich in wave power.

3.3.2 *Availability of wave energy resource*

To identify the spatial extent of resource abundance based on wave energy, the availability of wave energy resource is analyzed. The criterion for potential wave energy resource is that only a

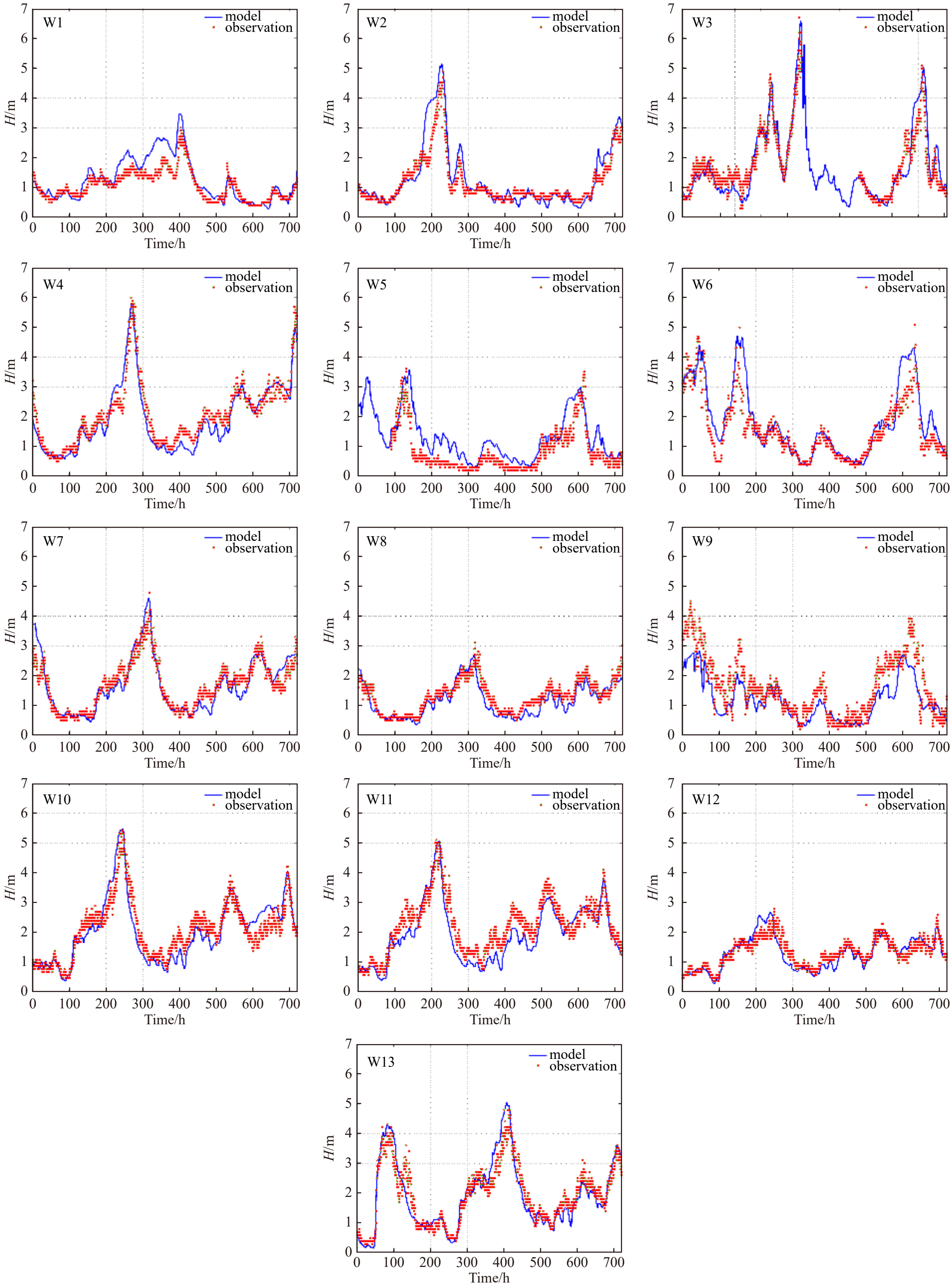

Fig. 2. Comparison between measured (dots) and modeled (curve) significant wave height (H_S) at the gauge stations W1–W13.

certain range of wave energy is considered, since too small wave energy is not sufficient to support continuous power generation, while excessive wave energy will damage the equipment and therefore cannot be used for power generation. However, there is no standard for defining the ranges of wave parameters for wave energy resource. In this study, waves with significant wave height of 1–4 m (Wan et al., 2015) and mean wave period greater than 2.5 s are assumed to be potential wave energy resource. Using the

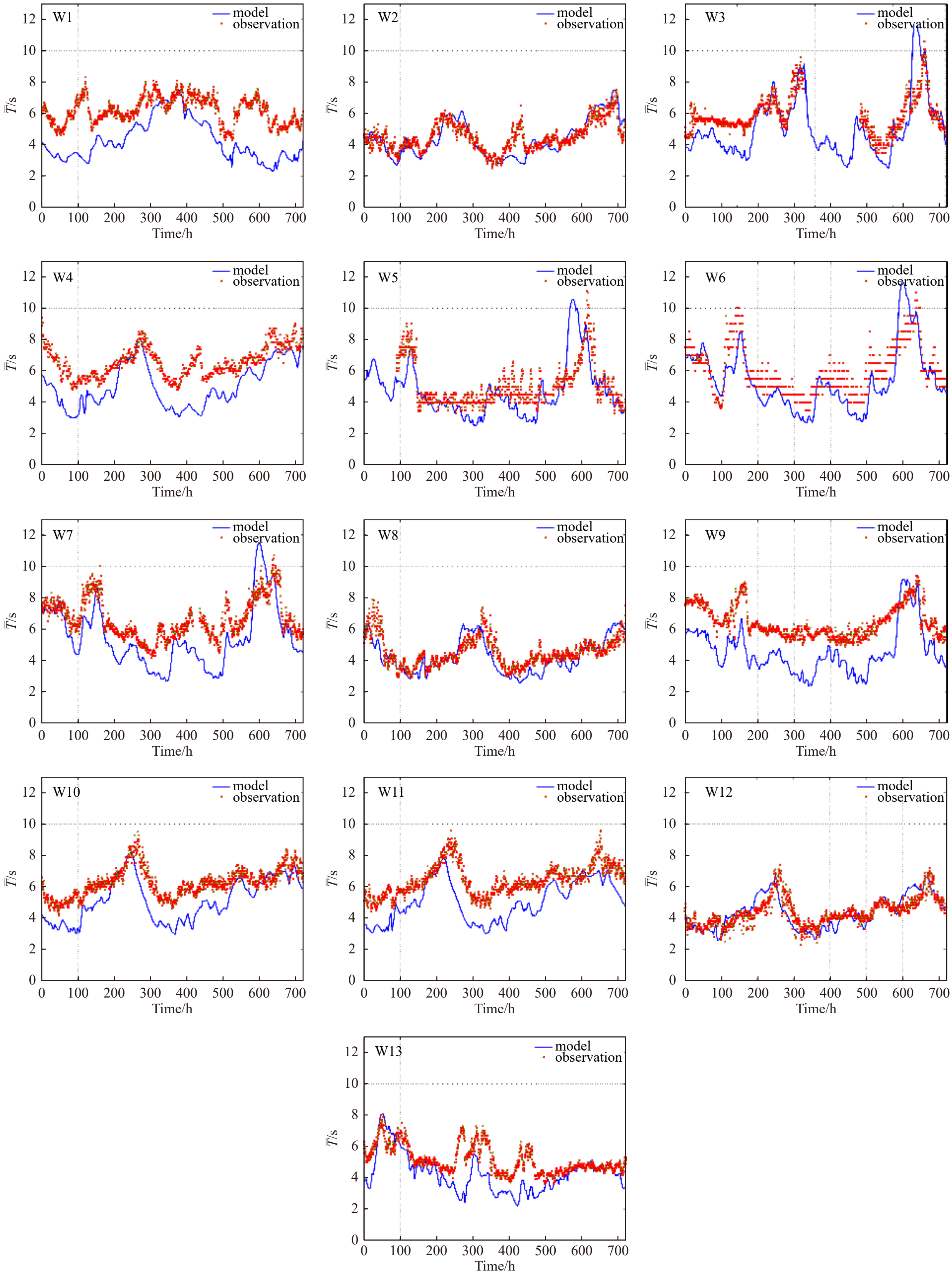

Fig. 3. Comparison between measured (dots) and modeled (curve) mean wave period ($\overline{T}$) at the gauge stations W1–W13.

numerical results of the 10 successive years, the duration that the wave is within the range, i.e., effective duration, was calculated for each year, and the annual average effective duration was obtained by averaging the effective duration of the 10 years. The annual average effective duration is used as an indicator to measure availability of wave energy resource.

Figure 7a shows the annual average effective duration of the sea areas, which, as a whole, tends to be longer in the open sea

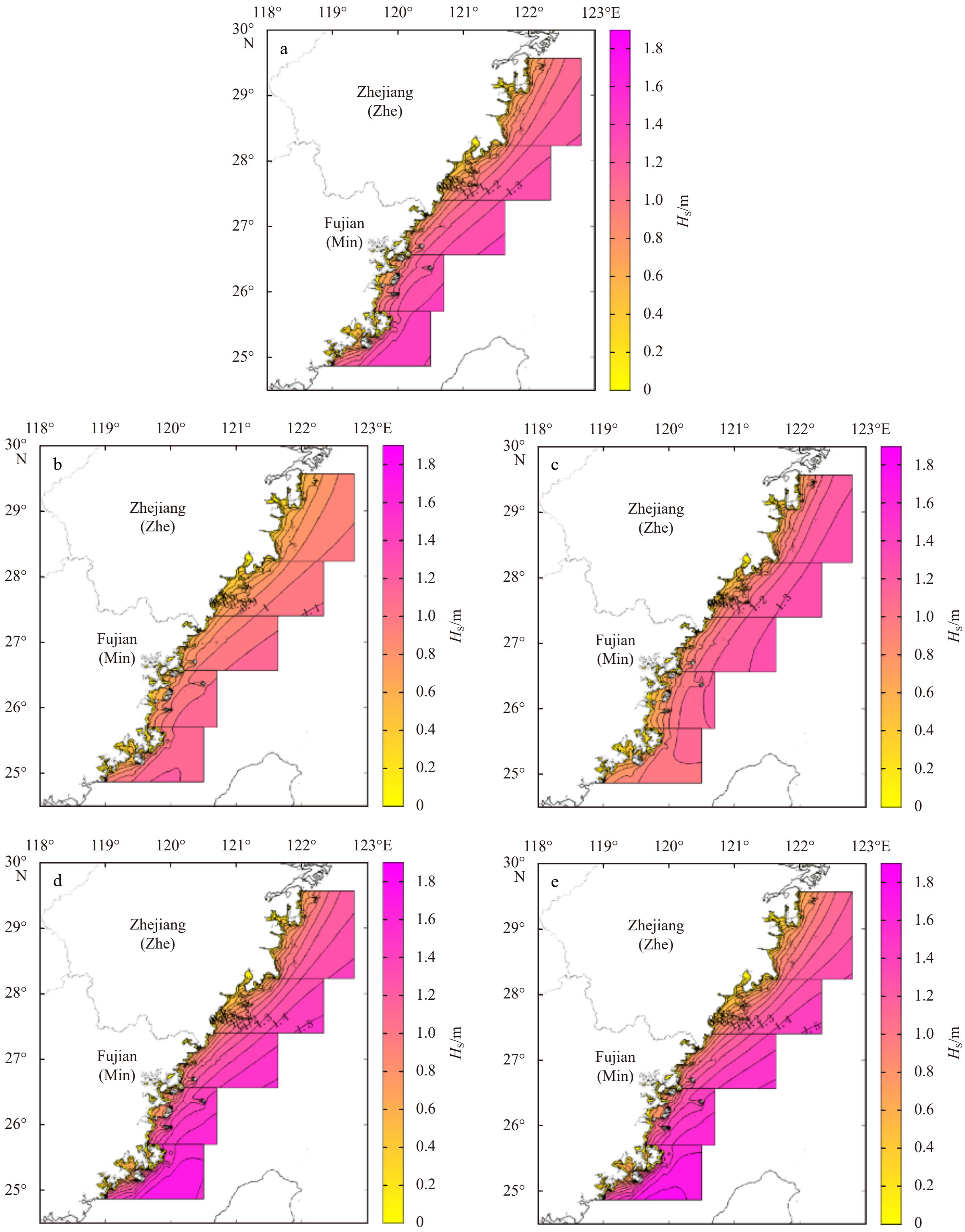

Fig. 4. Spatial distributions of annual average (a), spring (b), summer (c), autumn (d), and winter (e) significant wave height (H_S) .

and shorter in the coastal area, and to be longer in the south and shorter in the north (Table 2). When analyzing distribution patterns of the annual average effective duration, 1 500 h, 3 000 h and 5 000 h are chosen as dividing lines (Zhang et al., 2014). The sea area with effective duration more than 5 000 h shows that key areas D5 and D6 (in Zhejiang coastal area) contributed nearly zero, while key area D9 (in Fujian coastal area) accounts for 65.2%. For key areas D7 and D8 around the border between Zhejiang and Fujian provinces, values of effective duration mostly fall between 1 500 h and 5 000 h.

3.3.3 *Stability of wave energy resource*

To develop and utilize the wave energy, it is also necessary to know the stability of wave power density. Stable wave energy is more conducive to acquisition and conversion by development equipment. The coefficient of variation (COV) can reflect the stability of wave energy at each calculation point within the period of statistics; and the smaller the value is, the more stable the wave energy is. In case of short-term extreme weather that can trigger big waves, the COV will increase significantly, suggesting that the wave energy is not stable within that period. The formulation is as follows:

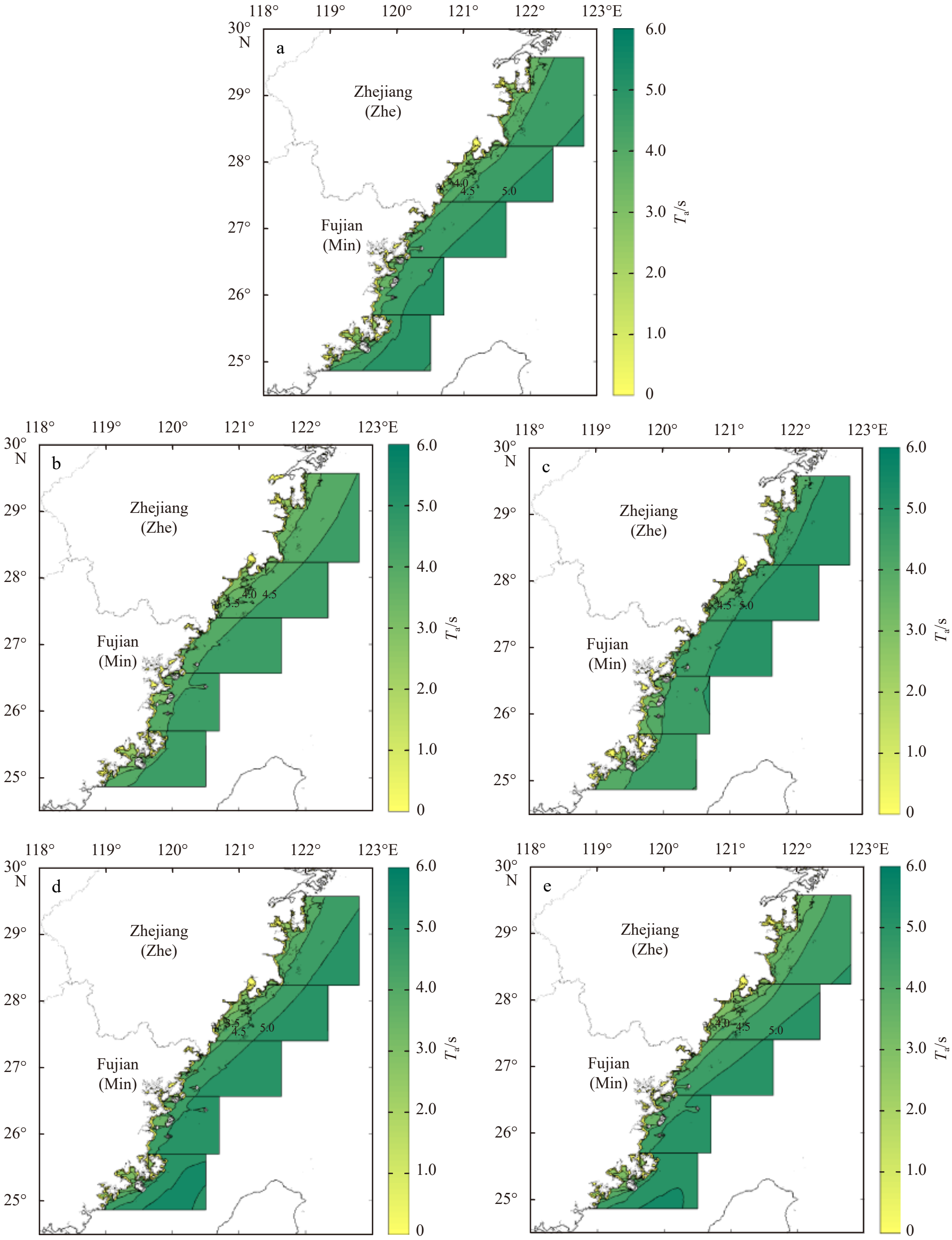

Fig. 5. Spatial distributions of annual average period $\overline{T}_a$(a), and average periods in spring (b), summer (c), autumn (d), and winter (e).

$$\mathrm{COV}(i,j)=\frac{1}{\overline{P}_W(i,j)}\sqrt{\frac{1}{N-1}\left[\sum_{t=1}^{N}P_W^{2}(i,j,t)-\frac{1}{N}\left(\sum_{t=1}^{N}P_W(i,j,t)\right)^{2}\right]},\tag{3}$$

where P_W is wave power density. Statistical data show that the COV of wave power density of the study area tends to be smaller in nearshore area than in the open sea, and to be smaller in the south than in the north; and it is mostly in the range of 1.5–3.0 (Fig. 7b). It can be concluded that the wave energy resource in the Fujian coastal area is more stable than that in the Zhejiang coastal area, especially around the Pingtan Island and its southern area with COV value of <1.5.

3.3.4 *Energy level frequency*

In the development and utilization of wave energy resource, the frequency of different energy levels is an important measure for the richness of wave power resource. It is generally considered that wave power is available when its density is greater than 2 kW/m, and sea area with value of 20 kW/m is considered to be rich in wave power (Zheng et al., 2011). In this paper, statistical analysis is carried out to define domains of wave power density frequency of more than 2 and 20 kW/m, respectively (Figs 7c and d). More than 50% of the study area shows usable

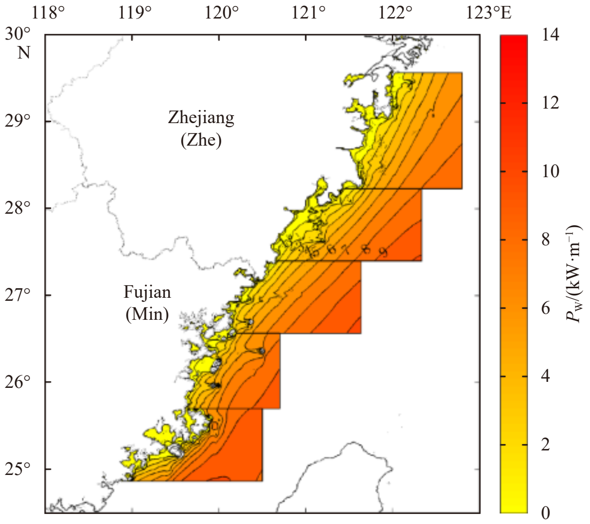

Fig. 6. Annual average wave power density.

level frequency, which are mostly located in the northern Zhejiang offshore area and southern Fujian coastal area especially around the Pingtan and Nanri Islands. Only less than 15% of the model domain is with rich level frequency, and this percentage is under 10% in the northern Zhejiang coastal area. Wave power resource is relatively rich in the southern Fujian coastal area, with value between 10% and 15%.

3.3.5 *Estimate of reserves of wave energy resource*

The wave power density refers to the wave energy passing the wave crest in a unit length (m), and the total wave energy can be obtained by integrating along the crest line. However, in natural sea conditions, we cannot carry out integration for an individual wave. Considering the randomness and stability of waves, we choose a suitable border line to integrate wave power density, to estimate the reserve N of wave energy resource in the offshore area:

$$N = \int P_{\mathrm{W}} \cdot \mathrm{d}L, \tag{4}$$

Table 1. Statistical results of annual average wave power density in each area

Key area	Spatial mean value/(kW · m^{-1})	Maximum/(kW · m^{-1})	$P_W \geqslant 2$ kW/m ratio/%	$P_W \geqslant 4$ kW/m ratio/%	$P_W \geqslant 6$ kW/m ratio/%
D5	5.3	8.9	87.0	71.0	47.0
D6	5.7	10.2	83.7	70.3	54.0
D7	6.6	10.4	93.8	82.8	65.2
D8	6.2	9.5	89.4	78.8	61.5
D9	7.0	10.1	87.0	79.7	70.3

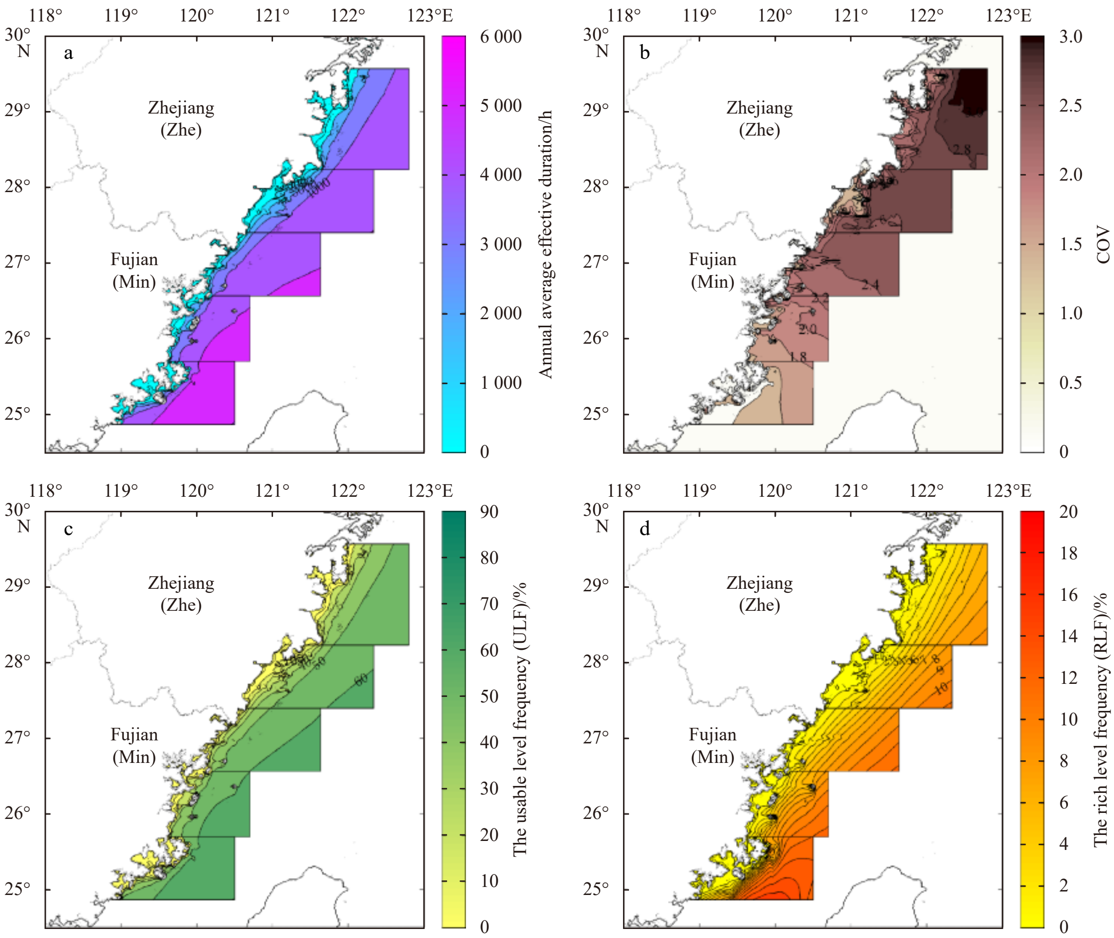

Fig. 7. Effective duration (a), coefficient of variation (b), usable level frequency (c), and rich level frequency (d) of wave energy.

Table 2. Statistical results of annual average effective duration in each area

Key area	Spatial mean value/h	Maximum/h	⩾1 500 h ratio/%	⩾3 000 h ratio/%	⩾5 000 h ratio/%
D5	3 518.1	4 784.7	90.0	76.8	0.0
D6	3 705.2	5 009.3	87.1	75.9	0.2
D7	4 286.2	5 135.7	95.6	90.1	13.1
D8	4 324.8	5 277.7	95.2	87.0	34.9
D9	4 450.5	5 350.3	89.0	85.8	65.2

where L refers to the length (m) of the border line.

In estimating the reserve of wave energy resource in this sea area, the border line is defined by the following two criteria: (1) in case that the distance between 20-m isobath and the shore is greater than 20 km, the 20-m isobath shall be selected; and (2) in case the distance between 20-m isobath and the shore is less than 20 km, the contour with the distance of 20 m from the shore shall be selected.

Statistical data show that the annual average total reserve of wave energy in the study area is 4.11×10^6 kW. In the period from June to September, the wave energy reserve in the northern areas is larger, which can be attributed to typhoon impact to a large extent. In the other months, the wave energy reserve in the southern areas is larger (Table 3). From the perspective of spatial distribution, the statistical reserve of the sea area is related to the length of wave crest line used for calculation; the energy per unit length is characterized by an increasing trend from the north to the south (Table 4).

Table 3. Statistics of monthly averaged reserve of wave energy in each key area (10^4 kW)

Key area	Jan.	Feb.	Mar.	Apr.	May	Jun.	Jul.	Aug.	Sept.	Oct.	Nov.	Dec.
D5	68	61	52	43	41	76	138	212	145	103	68	77
D6	58	54	44	37	34	62	118	139	109	85	59	63
D7	62	56	45	35	32	51	92	102	93	85	65	67
D8	85	72	56	38	32	40	62	75	89	107	91	90
D9	153	126	102	64	50	60	68	86	115	185	169	163

Table 4. Statistics of annual average reserve of wave energy in each key area

Key area	Annual average reserve of wave energy/(10^4 kW)	Length of wave crest line/km	Average wave power density along wave crest line/(kW·m^{-1})
D5	91	174.2	5.2
D6	72	131.0	5.5
D7	66	124.8	5.3
D8	70	117.1	6.0
D9	112	157.7	7.1
OE-W2	411	704.8	5.8

The statistical results obtained by Wang and Lu (2009) through general investigation showed that the total reserve of wave energy along Zhejiang and Fujian coasts is about 3.71×10^6 kW. Although their statistical method was rough estimation by replacing place with point, it is at present the most reliable one. The reserve of wave energy in OE-W2 accounts for 32% of the total value.

In recent years, estimates of the reserve of wave energy in each sea area have been provided by different methods, among them being Luo and Xia (2017) and Jiang et al. (2017), which estimated the reserve of wave energy in the East China Sea to be about 7.71×10^6 kW using the same method as the one used in this paper. In addition, Wang et al. (2016b) estimated the reserve of wave energy in Zhoushan sea area to be about 0.95×10^6kW using the 20-m isobath as the border line. Wang et al. (2013) estimated the reserve of wave energy in offshore areas of Zhejiang and Fujian to be about 1.79×10^6 kW and 1.67×10^6 kW, respectively, using the 30-m isobath as the border line.

Since the above energy reserves were estimated by different methods, it is not meaningful to carry out direct comparison. However, the estimated values show that they are of similar magnitude.

4 Conclusions

The wave energy resources in OE-W2 of the offshore areas of Fujian and Zhejiang were estimated and analyzed. The distributions of wave energy resources in the offshore areas were described in a relatively detailed manner using 10-year high-resolution numerical simulation of waves. The analysis gives the following findings:

(1) The sea area is rich in wave energy resource, which is not evenly distributed. The potential wave energy resource is up to 4.11×10^6 kW. In general, the potential wave energy in the south is more than that in the north. The annual average wave power density in most of the sea areas is more than 2 kW/m, but the wave energy is mainly distributed far from the shore, and it increases offshore.

(2) The surrounding of islands in the open sea is rich in wave energy resource, and the average wave power density around islands in the open sea is more than 4 kW/m. Such abundant wave energy resource provides a promising prospective for future development.

(3) As for the availability of wave energy, its distribution is consistent with the distribution of wave energy resource, and the effective duration increases from the coastal area to open sea.

(4) Due to the impact of frequent typhoons, the stability of wave energy in the study area is relatively poor. With regard to spatial distribution, the wave energy in the coastal area is more stable than that in the open sea, and wave energy in the southern part of the study region is more stable than that in northern part.

References

Ahn S, Haas K A, Neary V S. 2020. Wave energy resource characterization and assessment for coastal waters of the United States. Applied Energy, 267: 114922

Aboobacker V M, Shanas P R, Alsaafani M A, et al. 2017. Wave energy resource assessment for Red Sea. Renewable Energy, 114: 46–58

Arinaga R A, Cheung K F. 2012. Atlas of global wave energy from 10 years of reanalysis and hindcast data. Renewable Energy, 39(1): 49–64

Bingölbali B, Majidi A G, Akpınar A. 2021. Inter- and intra-annual wave energy resource assessment in the south-western Black Sea coast. Renewable Energy, 169: 809–819

Cai Xiaojie, Dai Jianhua, Zhu Zhihui, et al. 2019. Quality control and forecast verification of wind field in coastal waters of Shanghai. Meteorological Science and Technology (in Chinese), 47(2): 214–221

Chen Junwen, Cai Yang, Bai Yiping, et al. 2014. Simulation of one gale case in winter in the South China Sea. Marine Forecasts (in

Chinese), 31(4): 32–40
Goharnejad H, Nikaein E, Perrie W. 2021. Assessment of wave energy in the Persian Gulf: An evaluation of the impacts of climate change. Oceanologia, 63(1): 27–39
Gonçalves M, Martinho P, Soares C G. 2018. A 33-year hindcast on wave energy assessment in the western French coast. Energy, 165: 790–801
Gunn K, Stock-Williams C. 2012. Quantifying the global wave power resource. Renewable Energy, 44: 296–304
Jacobson P, Hagerman G. 2011. Mapping and assessment of the United States ocean wave energy resource. Palo, Alto, CA: EPRI
Jiang Bo, Ding Jie, Wu He, et al. 2017. Wave energy resource assessment along Bohai Sea, Yellow Sea and East China Sea. Acta Energiae Solaris Sinica (in Chinese), 38(6): 1711–1716
Kompor W, Ekkawatpanit C, Kositgittiwong D. 2018. Assessment of ocean wave energy resource potential in Thailand. Ocean & Coastal Management, 160: 64–74
Li Luping, Tian Suzhen, Xu Laisheng, et al. 1984. Power resource estimation of ocean surface waves in the Bohai Sea and Huanghai Sea and an evalution of prospects for converting wave power. Journal of Oceanography of Huanghai & Bohai Seas (in Chinese), 2(2): 14–23
Li Yongbo, Wu Kejian, Bi Fan, et al. 2013. Wave energy resources assessment in the Chengshan cape sea during the last 20 years by using SWAN wave model. Transactions of Oceanology and Limnology (in Chinese), (3): 1–9
Lin Yifan, Dong Sheng, Wang Zhifeng, et al. 2019. Wave energy assessment in the China adjacent seas on the basis of a 20-year SWAN simulation with unstructured grids. Renewable Energy, 136: 275–295
Luo Xuye, Xia Dengwen. 2017. Resource Characteristics and Evaluation Analysis of Ocean Energy in Offshore Key Areas of China (in Chinese). Beijing: China Ocean Press, 247
Ma Huaishu, Yu Qingwu. 1983. The preliminary eastimate for the potential surface wave energy resources in the adjacent sea areas of China. Marine Science Bulletin, 2(3): 73–81
Quitoras M R D, Abundo M L S, Danao L A M. 2018. A techno-economic assessment of wave energy resources in the Philippines. Renewable and Sustainable Energy Reviews, 88: 68–81
Ribal A, Babanin A V, Zieger S, et al. 2020. A high-resolution wave energy resource assessment of Indonesia. Renewable Energy, 160: 1349–1363
Rusu E, Onea F. 2019. A parallel evaluation of the wind and wave energy resources along the Latin American and European coastal environments. Renewable Energy, 143: 1594–1607
Shi Hongyuan, You Zaijin, Luo Xuye, et al. 2017. Assessment of wave energy resources for China Sea area based on 35 years' ERA-Interim reanalysis data. Transactions of Oceanology and Limnology (in Chinese), (6): 30–37
Wan Yong, Zhang Jie, Meng Junmin, et al. 2015. Exploitable wave energy assessment based on ERA-Interim reanalysis data—A case study in the East China Sea and the South China Sea. Acta Oceanologica Sinica, 34(9): 143–155
Wan Yong, Zheng Chongwei, Li Ligang, et al. 2020. Wave energy assessment related to wave energy convertors in the coastal waters of China. Energy, 202: 117741
Wang Chuankun. 1984. Primary analysis of the coastal wave energy source off China. Donghai Marine Science (in Chinese), 2(2): 32–38
Wang Zhifeng, Dong Sheng, Dong Xiangke, et al. 2016a. Assessment of wind energy and wave energy resources in Weifang sea area. International Journal of Hydrogen Energy, 41(35): 15805–15811
Wang Lvqing, Feng Weibing, Tang Xiaoning. 2013. Wave energy features of China's coastal provinces areas. Renewable Energy Resources, 31(11): 126–131
Wang Weiyuan, He Qianqian, Li Ruiyuan. 2016b. Assessment of wave energy resources in Zhoushan Sea. Water Power (in Chinese), 42(1): 93–97
Wang Chenghai, Hu Ju, Jin Shuanglong, et al. 2011. Application and test of lower level wind field simulation with Meso-scale model WRF in western region of Northwest China. Journal of Arid Meteorology (in Chinese), 29(2): 161–167
Wang Chuankun, Lu Wei. 2009. Analysis Method and Reserve Evaluation of Ocean Energy Resources (in Chinese). Beijing: China Ocean Press, 113
Ye Qin, Yang Zhongliang, Shi Weiyong, 2012. A preliminary study of the wave energy resources in the sea adjacent to Zhejiang. Journal of Marine Sciences (in Chinese), 30(4): 13–19
Zhang Rong, Jiang Bo, Zhang Song, et al. 2014. Application of wave energy development and utilization selection method in key exploration area of OE-W01. Ocean Development and Management (in Chinese), (9): 33–39
Zhang Jun, Xu Jindian, Guo Xiaogang. 2012. An evaluation and analysis of the ocean wave energy resource in nearshore waters of Fujian. Journal of Oceanography in Taiwan Strait (in Chinese), 31(1): 130–135
Zheng Chongwei, Li Xunqiang. 2011. Wave energy resources assessment in the China Sea during the last 22 years by using WAVEWATCH-Ⅲ wave model. Periodical of Ocean University of China (in Chinese), 41(11): 5–12
Zheng Chongwei, Zheng Yuyan, Chen Hongchun. 2011. Research on wave energy resources in the northern South China Sea during recent 10 years using SWAN wave model. Journal of Subtropical Resources and Environment (in Chinese), 6(2): 54–59